SYNTHESIS OF PRUSSIAN BLUE ANALOGUES OF $A_3[Fe(CN)_6]_2$ (A: Cu^{3+}, Co^{3+}, and Ni^{3+}) NANOPARTICLES AND APPLICATION IN THE ADSORPTION OF Cs^+, Sr^{2+}, AND Co^{2+}

***Lê Thị Hà Lan*[1,2]**
***Nguyễn Đình Trung*[2]**
***Trương Văn Minh*[3]**
***Lê Trần Minh Nhật*[4]**

ABSTRACT

The nuclear power plants and the research nuclear reactors have caused a large amount of radioactive waste in the environment, especially the nuclear reactor waste moves outward the water and atmospheric environment, which brings with it the risk of severe impact on the life of humans in the event of a nuclear accident. In this investigation, we have successfully prepared Prussian Blue analogues (PBAs) ($A_3[Fe(CN)_6]_2$ with different cations: $Cu_3[Fe(CN)_6]_2$, $Co_3[Fe(CN)_6]_2$, and $Ni_3[Fe(CN)_6]_2$. The synthesized PBAs were characterized and employed for the removal of Cs^+, Sr^{2+}, and Co^{2+} as sorption material samples, which are usually found in fission nuclear reactions in the nuclear reactor. Mostly, those sorption examinations reveal that $Cu_3[Fe(CN)_6]_2$ has the highest sorption capacity towards Cs^+ and Co^{2+} compared with those of $Co_3[Fe(CN)_6]_2$ and $Ni_3[Fe(CN)_6]_2$; $Co_3[Fe(CN)_6]_2$ has higher sorption capacity towards Sr^{2+} than those of $Cu_3[Fe(CN)_6]_2$ and $Ni_3[Fe(CN)_6]_2$. These findings are important since they can enable rational the design of sorbents with suitable ion exchange capacity and selectivity toward targeted radioactive wastes.

Keywords: *Cesium, Strontium, Cobalt, Prussian Blue sorption, radioactive waste*

1. Introduction

In recent years, there have been several classes of porous inorganic materials that match the aforementioned standards, such as clays [1], zeolites [2], Prussian blue (PB), and Prussian blue analogues (PBAs) [3]. Such materials exhibit high porosity, excellent thermal and radiation stability [4], which render them highly applicable in many fields, including information/energy storage [5], and radioactive waste removal [6].

In this research, we successfully synthesized different PBAs, including $A_3[Fe(CN)_6]_2$ (A: Cu^{3+}, Co^{3+}, and Ni^{3+}) and applied theirs adsorption performances with Cs^+, Sr^{2+}, and Co^{2+} ions. It was found that the substitution of the transition metal ions used (Cu^{3+}, Co^{3+}, and Ni^{3+}) in the structure of PBAs led to improved adsorption capacity and selectivity. Total reflection X-ray fluorescence spectroscopy analysis (TXRF) provides quantitative evidence with respect to the adsorption mechanism of the obtained PBAs.

2. Materials and methods

2.1. Materials

Standard solutions (Cs^+ (1000 mg/L), Sr^{2+} (1000 mg/L), Co^{2+} (1000 mg/L)), CsCl (99.99%, Meck), $SrCl_2$ (99.99%, Meck), $CoCl_2$ (99.99%, Meck), $K_4[Fe(CN)_6]$ (99.99%, Meck), $CoCl_2$. $6H_2O$ (99.99%, Meck), $CuCl_2$. $2H_2O$ (99.99%, Meck), and $NiSO_4$. $6H_2O$ (99.99%, Meck) were used as received. pH are adjusted using HNO3 (0.01 – 0.1N) and NaOH (0.01–0.1N).

2.2. Synthesis of $A_3[Fe(CN)_6]_2$

The synthetic protocol for $A_3[Fe(CN)_6]_2$ (A = Co, Cu, and Ni) was modified from previous reports [7]. For

[1]Trường THPT Trần Phú, Đà lạt
Email: hoalantigon2006@gmail.com
[2]Trường Đại học Đà lạt
[3]Trường Đại học Đồng Nai
[4]Viện Liên hiệp nghiên cứu hạt nhân Dubna (JINR)

the synthesis of $Co_3[Fe(CN)_6]_2$, a 250 mL of 0.05 M $K_3[Fe(CN)_6]$ solution was slowly added to a 750 mL of 0.15 M $CoCl_2$ solution. The reaction mixture was stirred at 1200 rpm and sonicated, prior to heating to 60^0C for four hours. Upon reaction completion, the product was purified by repeated washing with water and centrifugation, and dried at 70^0C. For the synthesis of $Cu_3[Fe(CN)_6]_2$ and $Ni_3[Fe(CN)_6]_2$, a $CuCl_2$ or $NiSO_4$ solution is used respectively in place of $CoCl_2$ in the aforementioned procedure. The other reaction conditions remained unchanged.

2.3. Adsorption performance of $A_3[Fe(CN)_6]_2$ towards Cs^+, Sr^{2+}, and Co^{2+}

Cs^+, Sr^{2+}, and Co^{2+} used in this study are stable isotopes. A series of reaction flaks containing 50 mL of Cs^+, Sr^{2+}, and Co^{2+} solution with concentrations of 0.1 mg/L, 1 mg/L, 10 mg/L, 30 mg/L, 50 mg/L, 70 mg/L, 100 mg/L, 150 mg/L, 200 mg/L, 250 mg/L, 300 mg/L, 350 mg/L, 400 mg/L, 450 mg/L were prepared. To the above solutions, 0.1g of the as-synthesized $A_3[Fe(CN)_6]_2$ was added. The pH was adjusted to 7.0 and the mixture was sealed and shaken at 270 times/min for 24 hours at 25^0C in order to reach equilibrium. After adsorption completion, the adsorbents were separated by centrifugation (8500 rpm, 10 min), and the remaining solution was filtered through a 220 nm filter for further analysis with TXRF.

The adsorption capacity of $A_3[Fe(CN)_6]_2$ toward Cs^+, Sr^{2+}, and Co^{2+} is calculated by the following formula:

$$q = \frac{V \times (C_i - C_e)}{B} \quad (1)$$

where q is the adsorption capacity of the material (mg/g adsorbent); C_i and C_e are the concentrations of Cs^+, Sr^{2+}, and Co^{2+} before and after adsorption, respectively; V is the volume of the solution; B is the mass of the asorbent used.

Langmuir and Freunlich models were used to assess the adsorption performance of $A_3[Fe(CN)_6]_2$.

Langmuir adsorption equation

$$q_e = \frac{Q_m \times b \times C_e}{1 + bC_e} \quad (2)$$

where q_e is the amount of Cs^+, Sr^{2+}, and Co^{2+} ions adsorbed by the material (mg/g), Q_m: maximum adsorption capacity of ions; C_e is the initial concentration at a point of adsorption (mg/L); rate constant b: adsorption/desorption.

Freunlich adsorption equation

$$q_e = K \times C_e^{1/n} \quad (3)$$

where q_e is the amount of Cs^+, Sr^{2+}, and Co^{2+} ions adsorbed by the material (mg/g); K and n are the adsorption constant at equilibrium.

2.4. TXRF analyses of the Cs^+, Sr^{2+}, and Co^{2+} concentration

After adsorption completion, the adsorbents were washed several times with distilled water, and dried at 60^0C. The sample elemental contents were analyzed by total reflection X-ray fluorescence (TXRF) to monitor the change in the composition of the material before and after the reaction. The content of Cs^+, Sr^{2+}, and Co^{2+} before and after adsorption remaining in the solution was also measured by TXRF.

2.5. Characterizations

Crystalline structures of $A_3[Fe(CN)_6]_2$ were investigated by powder X-ray diffraction (PXRD) performed with a Bruker D8 Advance

diffractometer using Cu Kα radiation (wavelength 1.541 Å) in focused beam and in the range 10-80^0. The morphologies of $A_3[Fe(CN)_6]_2$ were imaged using field emission transmission electron microscopy (FE-TEM; JEM 2100 - Jeol, Japan). The composition of the material before and after the reaction was analyzed using total reflection X-ray fluorescence (TXRF) S2 Picofox Bruker.

3. Results and discussions

$A_3[Fe(CN)_6]_2$ was readily synthesized by precipitating Cu^{3+}, Co^{3+}, and Ni^{3+} salt with $K_3[Fe(CN)_6]$ aqueous solution at 60 ^{0}C for four hours. The chemical reactions for $A_3[Fe(CN)_6]_2$ are as follows:

$3NiSO_4 + 2K_3[Fe(CN)_6] \rightarrow Ni_3[Fe(CN)_6]_2 + 3K_2SO_4$ (4)

$3CuCl_2 + 2K_3[Fe(CN)_6] \rightarrow Cu_3[Fe(CN)_6]_2 + 6KCl$ (5)

$3CoCl_2 + 2K_3[Fe(CN)_6] \rightarrow Co_3[Fe(CN)_6]_2 + 6KCl$ (6)

Crystalline properties of the as-synthesized $A_3[Fe(CN)_6]_2$ were examined using XRD, and the data are shown in Figure 1. As seen, $Ni_3[Fe(CN)_6]_2$, $Co_3[Fe(CN)_6]_2$, and $Cu_3[Fe(CN)_6]_2$ with their crystallographic patterns JCPDS No: 14-291, 15-0806, and 03-0513, respectively, exhibit a high degree of crystallinity with characteristic diffraction peaks located at 2θ from 10^0 ÷ 80^0, which correspond to the facets (200), (220), (400), (420), (422), (440), (620), and (622).

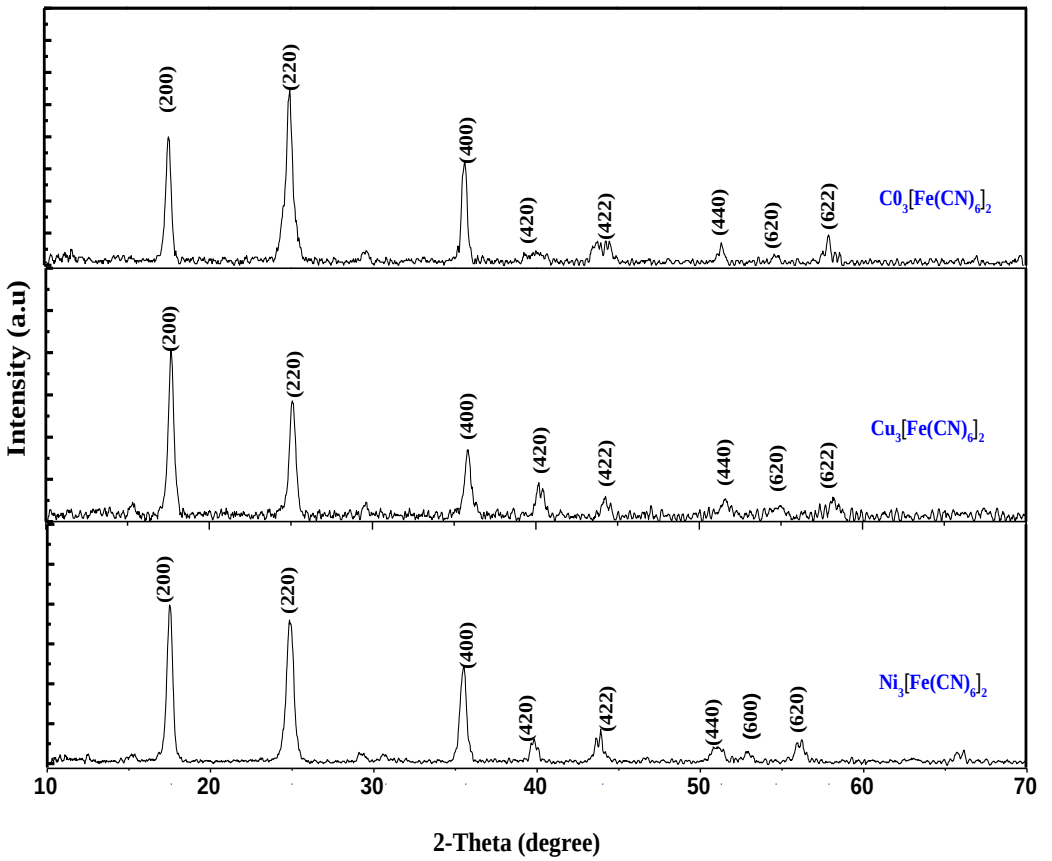

Figure 1: *PXRD of $A_3[Fe(CN)_6]_2$ (A: Co, Cu, Ni)*

The particle size and morphological characteristics of $A_3[Fe(CN)_6]_2$ were examined using transmission electron microscopy (TEM) (Figure 2). As seen, $Co_3[Fe(CN)_6]_2$ shows pseudo-spherical shape with the average size varying between 20 and 80 nm (Figure 2a), $Cu_3[Fe(CN)_6]_2$ is between 60 and 120 nm (Figure 2b), and $Ni_3[Fe(CN)_6]_2$ is between 15 and 35 nm (Figure 2c).

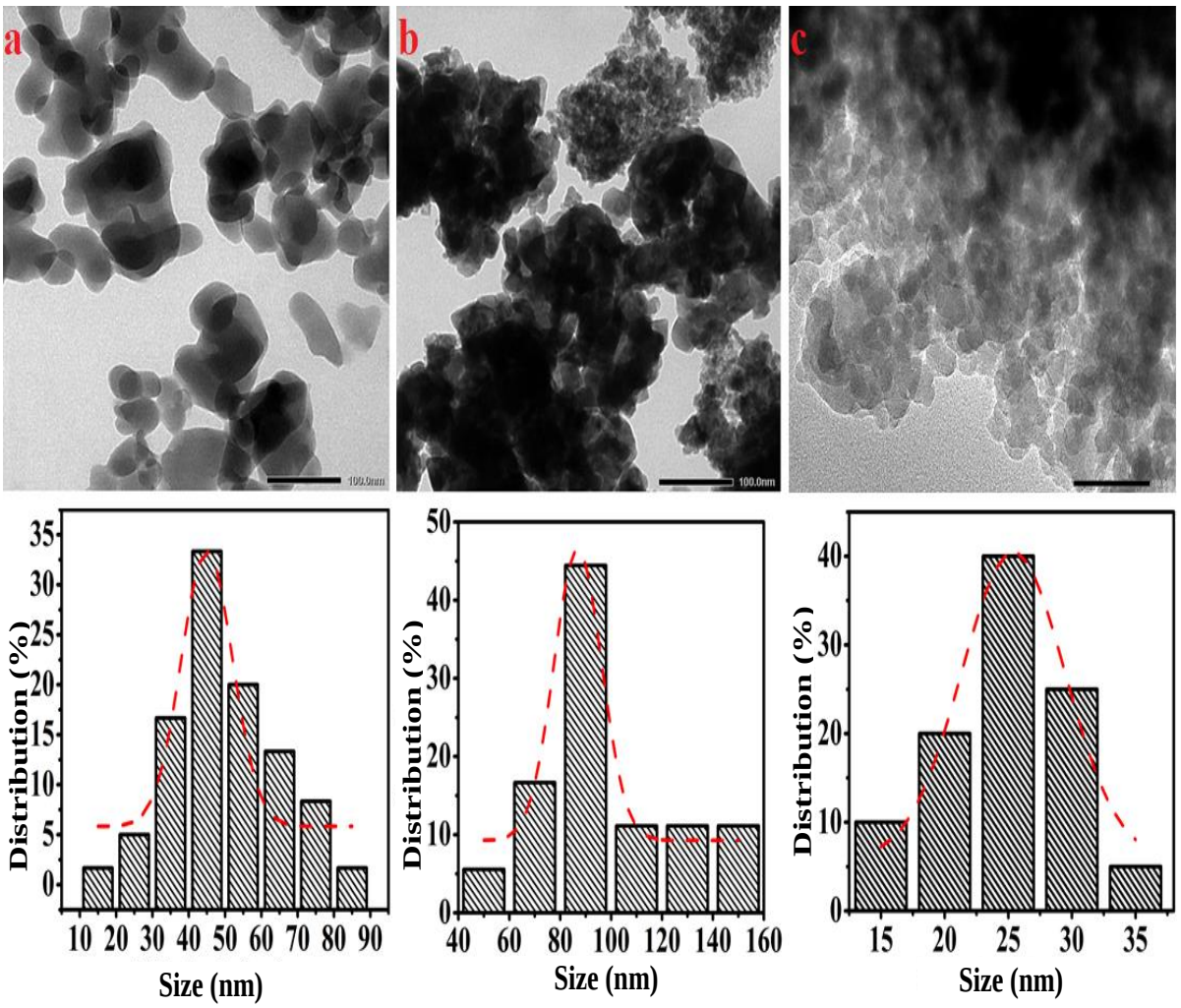

Figure 2: *TEM images and the corresponding particle size distribution of (a) $Co_3[Fe(CN)_6]_2$, (b) $Cu_3[Fe(CN)_6]_2$, and (c) $Ni_3[Fe(CN)_6]_2$*

Although there have been a number of publications demonstrating adsorption performance of PBAs towards individual radioactive nuclides Cs^+, Sr^{2+}, and Co^{2+} (Table 1), there is little research comparing the adsorption capacity of Cs^+, Sr^{2+}, and Co^{2+} ions and the correlation between PBA compositions and adsorption activities.

Table 1: *Comparison of the adsorption capacity of Cs^+, Sr^{2+}, and Co^{2+} ions on different adsorbent materials*

Adsorbent	pH	Maximum adsorption capacity (mg g−1)	References
Cs^+ Ion			
Copper hexacyanoferrate(CuHCF)	7.0	111.65	This research
Cobalt hexacyanoferrate(CoHCF)	7.0	44.24	This research
Nickle hexacyanoferrate(NiHCF)	7.0	40.60	This research
Zeolite A	6.0	208.7	[8]
Ammonium molybdophosphate-polyacrylonitrile	6.5	81.3	[9]
Prussian Blue/Fe_3O_4	7.0	280.82	[10]
MOF/KNiFC	5.0	153	[11]
Sr^{2+} Ion			
Copper hexacyanoferrate(CuHCF)	7.0	23.69	This research
Cobalt hexacyanoferrate(CoHCF)	7.0	37.07	This research
Nickle hexacyanoferrate(NiHCF)	7.0	4.19	This research
Carboxymethylated cellulose	4.0	108.7	[12]
ZrP-SO_3H	4.0	183.21	[13]
Co^{2+} Ion			
Copper hexacyanoferrate(CuHCF)	7.0	41.83	This research
Nickle hexacyanoferrate(NiHCF)	7.0	25.16	This research
Silica SBA-15		181.67	[14]
Ordered Micro- and Mesoporous/SiO_2		8.43	[15]
GO-NH_2		116.35	[16]

The adsorption isotherms of $A_2[Fe(CN)_6]$ towards Cs^+, Sr^{2+}, and Co^{2+} were examined at 25 ºC and pH 7. The parameters of the isothermal adsorption of Cs^+, Sr^{2+}, and Co^{2+} ions on $A_3[Fe(CN)_6]_2$ estimated from Langmuir and Freudlich models are shown in Table 2. It is interesting to note that $Cu_3[Fe(CN)_6]_2$ shows much higher maximum adsorption capacity (Q_m) towards Cs^+ (111.65 mg g^{-1}) and Co^{2+} (41.83 mg g^{-1}) than those of PBAs, while $Co_3[Fe(CN)_6]_2$ absorbed Sr^{2+} higher adsorption capacity than $Cu_3[Fe(CN)_6]_2$ and $Ni_3[Fe(CN)_6]_2$.

Table 2: *Adsorption isothermal parameters of Cs^+, Sr^{2+}, and Co^{2+} by $A_3[Fe(CN)_6]_2$ extract from Langmuir and Freundlich models*

Langmuir					Freundlich		
Ion	**Adsorbent material**	**Q_m (mg/g)**	**K_L (L/mg)**	**R^2**	**K_F (mg/g)**	**n**	**R^2**
Cs^+	$Cu_3[Fe(CN)_6]_2$	111.65	2.094	0.925	61.99	8.094	0.893
	$Co_3[Fe(CN)_6]_2$	44.24	0.015	0.953	6.49	3.357	0.843
	$Ni_3[Fe(CN)_6]_2$	40.60	0.259	0.879	21.06	8.490	0.930
Sr^{2+}	$Cu_3[Fe(CN)_6]_2$	23.69	0.017	0.968	2.579	2.797	0.925
	$Co_3[Fe(CN)_6]_2$	37.07	0.006	0.978	1.303	1.964	0.949
	$Ni_3[Fe(CN)_6]_2$	4.19	0.022	0.920	0.642	3.280	0.927
Co^{2+}	$Cu_3[Fe(CN)_6]_2$	41.83	0.049	0.960	9.354	3.855	0.927
	$Ni_3[Fe(CN)_6]_2]$	25.16	0.008	0.955	1.346	2.223	0.902

In order to further understand the sorption mechanism, TXRF was used to investigate the solution composition before and after sorption (Figure 3). Figures 3a, 3b, and 3c demonstrate the characteristic peaks of Cs^+ (4.3 keV), Sr^{2+} (14.2 keV), and Co^{2+} (6.93 keV) of the solution after sorption by $A_2[Fe(CN)_6]_3$. After the sorption reaches equilibrium, the peak intensity corresponding to Cs^+, Sr^{2+}, and Co^{2+} decreases, revealing the sorption process of those cations by the PBAs.

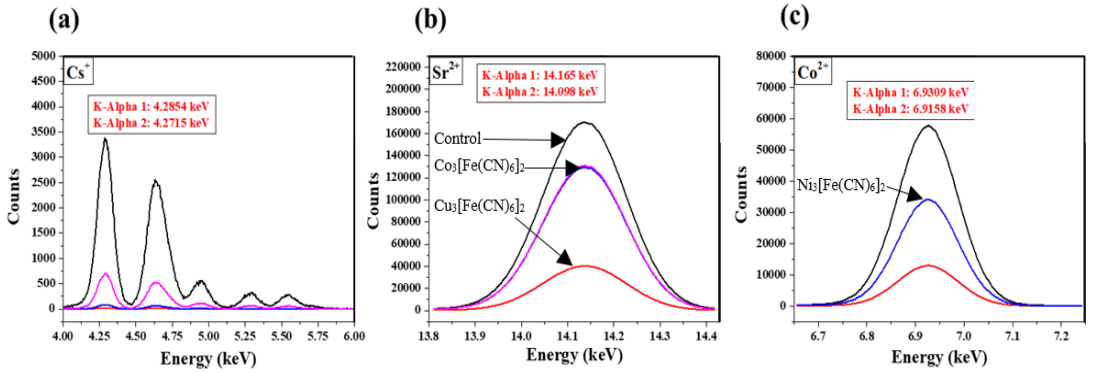

Figure 3: *TXRF spectra analyzing the composition of the waste solution before and after adsorption by $A_3[Fe(CN)_6]_2$*

4. Conclusion

Prussian blue analogues (PBAs) with different substituted cations ($A_3[Fe(CN)_6]_2$ (A: Cu^{3+}, Co^{3+}, and Ni^{3+})) were successfully synthesized and applied for the removal of Cs^+, Sr^{2+}, and Co^{2+}. This research was shown that $Cu_3[Fe(CN)_6]_2$ exhibits the higher sorption capacity towards Cs^+, and Co^{2+} compared with those of $Co_2[Fe(CN)_6]$ and $Ni_2[Fe(CN)_6]$; for Sr^{2+} case, $Co_3[Fe(CN)_6]_2$ exhibits a little higher sorption capacity compared with $Cu_3[Fe(CN)_6]_2$ and around 6 times higher sorption capacity compared with $Ni_3[Fe(CN)_6]_2$. TXRF data reveal that the cation exchange ability of substituted metal within the framework of PBAs has a significant impact on the sorption performance of PBAs. In addition, the similarity between Cs^+ size and the channel window size of PBAs leads to a preferential sorption of Cs^+ over Sr^{2+} and Co^{2+}.

REFERENCES

1. A. F. Seliman, Y. F. Lasheen, M. A. E. Youssief, M. M. Abo-Aly & F. A. Shehata (2014), "Removal of some radionuclides from contaminated solution using natural clay: bentonite", *Journal of Radioanalytical and Nuclear Chemistry*, 300(3), pp. 969-979

2. Kubota, T., Fukutani, S., Mahara, Y. (2013), "Removal of radioactive cesium, strontium, and iodine from natural waters using bentonite, zeolite, and activated carbon", *Journal of Radioanalytical and Nuclear Chemistry*, 296(2), pp. 981-984

3. De Tacconi, Norma R, Rajeshwar, Krishnan, and Lezna, Reynaldo O (2003), "Metal hexacyanoferrates: electrosynthesis, in situ characterization, and applications", *Chemistry of Materials*, 15(16), pp. 3046-3062

4. Denton, Mark S, Manos, Manolis J, and Kanatzidi, Mercouri G (2009), "Highly Selective Removal of Cesium and Strontium Utilizing a New Class of Inorganic Ion Specific Media–92670", *Northwestern University, Department of Chemistry*, 2145,

pp. 60208-3113

5. Briana Aguila, Debasis Banerjee, Zimin Nie, Yongsoon Shin, Shengqian Ma, Praveen K Thallapally (2016), "Selective removal of cesium and strontium using porous frameworks from high level nuclear waste", *Chemical Communications*, 52(35), pp. 5940-5942

6. Catala, Laure and Mallah, Talal (2017), "Nanoparticles of Prussian blue analogs and related coordination polymers: From information storage to biomedical applications", *Coordination Chemistry Reviews*, 346, pp. 32-61

7. Tingting Li, Fan He, YaoDong Dai (2016), "Prussian blue analog caged in chitosan surface-decorated carbon nanotubes for removal cesium and strontium", *J Radioanal Nucl Chem*, 310, pp.1139–1145

8. Itaya, Kingo, Uchida, Isamu, and Neff, Vernon D (1986), "Electrochemistry of polynuclear transition metal cyanides: Prussian blue and its analogues", *Accounts of Chemical Research*, 19(6), pp. 162-168

9. El-Kamash, AM (2008), "Evaluation of zeolite A for the sorptive removal of Cs^+ and Sr^{2+} ions from aqueous solutions using batch and fixed bed column operations", *Journal of hazardous materials*, 151(2-3), pp. 432-445

10. Nagy L. Torad, Ming Hu, Masataka Imura, Yusuke Yamauchi (2012), "Large Cs adsorption capability of nano-structured Prussian Blue particles with high accessible surface areas. *Journal of Materials Chemistry*, 22(35), pp. 18261-18267

11. Naeimi, Shakiba and Faghihian, Hossein (2017), "Performance of novel adsorbent prepared by magnetic metal-organic framework (MOF) modified by potassium nickel hexacyanoferrate for removal of Cs^+ from aqueous solution", *Separation and Purification Technology*, 175, pp. 255-265

12. Hossein Faghihiana, Mozhgan Iravania, Mohammad Moayeda, Mohammad Ghannadi, (2013), "Preparation of a novel PAN–zeolite nano-composite for removal of Cs^+ and Sr^{2+} from aqueous solutions: Kinetic, equilibrium, and thermodynamic studies", *Chemical engineering journal*, 222, pp. 41-48

13. Wanjun Mu, Shenzhen Du, Qianhong Yu, Xingliang Li, Hongyuan Wei, YuchuanYang, Shuming Peng (2019), "Highly efficient removal of radioactive ^{90}Sr based on sulfonic acid-functionalized α-zirconium phosphate nanosheets", *Chemical Engineering Journal*, 361, pp. 538-546

14. Wenlu Guo, Rui Chen, Yan Liu, Minjia Meng, Xiangguo Meng, Zhaoyong Hu, Zhilong Song (2013), "Preparation of ion-imprinted mesoporous silica SBA-15 functionalized with triglycine for selective adsorption of Co(II)", *Colloids and Surfaces A: Physicochemical and Engineering Aspects*, 436, pp. 693-703

15. Jenny Andersson, Jessica Rosenholm, Sami Areva, and Mika Lindén (2004), "Influences of material characteristics on ibuprofen drug loading and release profiles from ordered micro-and mesoporous silica matrices", *Chemistry of Materials*, 16(21),

pp. 4160-4167

16. Fang Fang, Lingtao Kong, Jiarui Huang, Shibiao Wu, Kaisheng Zhang, Xuelong Wang, Bai Sun, Zhen Jin, Jin Wang, Xing-Jiu Huang, Jinhuai Liu (2014), "Removal of cobalt ions from aqueous solution by an amination graphene oxide nanocomposite", *Journal of Hazardous Materials*, 270, pp. 1-10

TỔNG HỢP VẬT LIỆU NANO NHÓM PRUSSIAN BLUE $A_3[Fe(CN)_6]_2$ (A: Cu^{3+}, Co^{3+}, VÀ Ni^{3+}) VÀ ỨNG DỤNG TRONG HẤP THU CÁC ION Cs^+, Sr^{2+}, VÀ Co^{2+}

TÓM TẮT

Nhà máy điện hạt nhân và các lò phản ứng hạt nhân nghiên cứu đã tạo ra một lượng lớn chất thải phóng xạ trong môi trường, đặc biệt là chất thải phóng xạ này di chuyển ra ngoài môi trường nước và môi trường không khí, làm cho ảnh hưởng nghiêm trọng đến đời sống của con người ở các sự cố hạt nhân. Trong nghiên cứu này, chúng tôi đã điều chế thành công các Prussian Blue (PBAs) $A_3[Fe(CN)_6]_2$ gồm: $Cu_3[Fe(CN)_6]2$, $Co_3[Fe(CN)_6]2$, và $Ni_3[Fe(CN)_6]_2$. Các PBAs đã được tổng hợp và ứng dụng chúng để hấp thu và loại bỏ các ion Cs^+, Sr^{2+} và Co^{2+}, đây là những đồng vị phóng xạ được tìm thấy trong phản ứng phân hạch của lò phản ứng hạt nhân. Hầu hết các phép thử nghiệm về hấp phụ cho thấy, đối với Cs^+ và Co^{2+} thì $Cu_3[Fe(CN)_6]_2$ có khả năng hấp phụ cao hơn so với $Co_3[Fe(CN)_6]_2$ và $Ni_3[Fe(CN)_6]_2$; còn $Co_3[Fe(CN)_6]_2$ có khả năng hấp phụ Sr^{2+} cao hơn $Cu_3[Fe(CN)_6]_2$ và $Ni_3[Fe(CN)_6]_2$. Những phát hiện này rất quan trọng vì chúng cho phép chọn lựa hợp lý các chất hấp thu để hấp thu các chất thải phóng xạ thông qua khả năng trao đổi ion và hấp phụ qua bề mặt.

Từ khóa: *Cesium, Stronti, Coban, chất hấp thu Prussian Blue, chất thải phóng xạ*

(Received: 28/6/2022, Revised: 13/7/2022, Accepted for publication: 31/8/2022)